Hong Kong International Journal of Research Studies, ISSN: 3078-4018
Volume 3, Issue 2, July-December, 2025
Available online at:https://octopuspublication.com/index.php/hkijrs

Experimenting with Grid-Connected Photovoltaic Systems Through Modeling and Simulation of Grid Inverters

Dr. Manjeet

Associate Professor, Electrical and Electronics Engineering Dept. Krishna Vidyapeeth of Management and Technology, Khera, Siwani Dist. Bhiwani, Haryana

ABSTRACT

This study develops MATLAB/Simulink inverter simulation models for grid-connected photovoltaic systems (GCPV). This work contributes to the development of a comprehensive GCPV system simulation model. Sunlight and temperature at the PV array feed the inverter simulation model, which outputs AC electricity. Phase-shift control synchronizes the inverter output with the utility grid at unity power factor. The model is tested using data from a 45.35 kWp GCPV system at the Malaysia Green Technology Corporation (MGTC) in Bangi, Malaysia. The model's validation is based on RMSE and MAPE. Simulation findings revealed that the inverter output power is adequate, with only minor variance from the actual data. The de-rating variables in this study were wrongly forecasted.

Keywords: Photovoltaic; Solar; Grid Inverter; Simulation; De-Rating Factor.

INTRODUCTION

A grid-connected photovoltaic system (GCPV) relies on a grid inverter to convert the DC electricity generated by the PV array into AC power that matches the grid's voltage and frequency. A typical GCPV system includes a PV array, MPPT unit(s), inverter, and utility grid, as shown in Fig. 1.

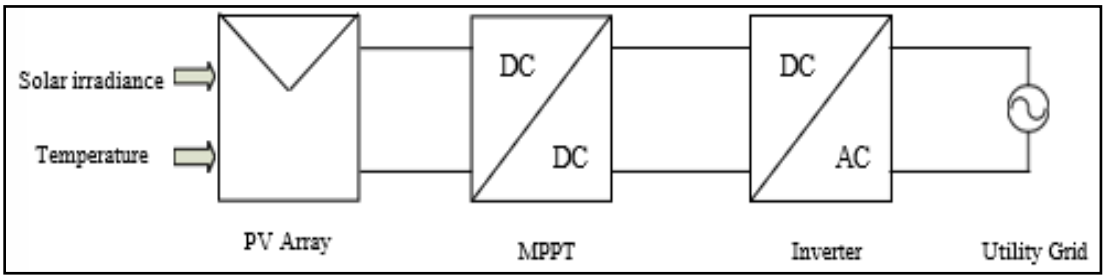

Figure 1: A Typical GCPV System Block Diagram

PV arrays generate DC electricity from sunshine. In practice, a PV array is coupled to an MPPT to maximize power output. Inverters transform DC power into AC power before sending it to the utility grid. MPPT is usually incorporated within the inverter. Grid inverters are different from stand-alone PV inverters. Grid inverters transmit current to the utility grid at a unity power factor, as specified in their main specifications. Some new inverters have adjustable power factors. Centralized, string, multi-string, and modular grid inverters are offered for PV applications [1-3]. Studies on modeling PV system components reveal that this approach is becoming increasingly essential in PV system development. Simulation software enables PV systems to be reviewed and examined without modifying the real system, thereby saving time and money. The creation of a complete GCPV system simulation model will include inverter modeling [4]. Comparing simulation output with data from an installed GCPV system at the Malaysia Green Technology Corporation (MGTC) in Bangi, Malaysia, validates the model. The 45.35 kWp GCPV system, also known as Pack A1, is installed.

METHODOLOGY

Inverter Design

MGTC's Pack A1 PV system uses centralized inverters. The centralized inverter design

Hong Kong International Journal of Research Studies, ISSN: 3078-4018
Volume 3, Issue 2, July-December, 2025
Available online at:https://octopuspublication.com/index.php/hkijrs

Table 1: Fronius IG500 Inverter Specs

	Subjects	Descriptions
Inputdata	Recommended power supply	40–52kWp
	MPP voltage range	210–420V
	Maximuminputvoltage	530 V
	Maximuminputcurrent	205 A
Outputdata	Nominal output power	40 kW
	Nominal frequency	50±0.2 Hz
	Distortion factor	<5%
	Powerfactor	1
Generaldata	Maximum efficiency	94.3%

This study models a single-phase full-bridge inverter. The semiconductor switch used is an IGBT, which can withstand a significant amount of power and is ideal for this PV system. Figure 2 depicts a schematic diagram of the designed grid inverter model for the GCPV system. The full-bridge inverter employs a bipolar switching mechanism and exhibits two distinct switching states, as outlined in Table 2. The PWM inverter's output waveform is then filtered to provide a sinusoidal AC waveform—schematic diagram for GCPV system.

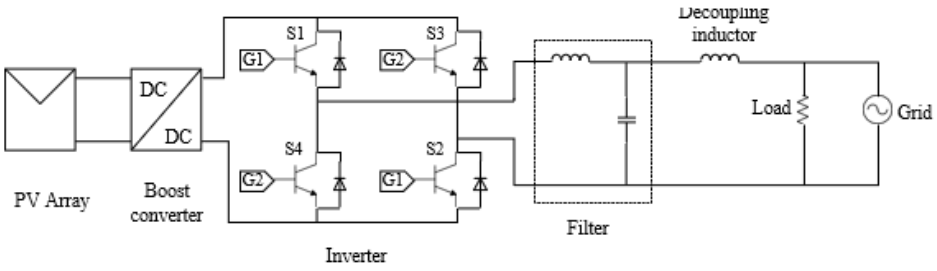

Figure 2: Inverter schematic illustration in a GCPV system

Table 2: Inverter State Transitions in a Single-Phase Full-Bridge Inverter

Switching State	Switches ON	Switches OFF
1	S1,S2	S3,S4
2	S3,S4	S1,S2

IPBT gates are driven by sinusoidal PWM (SPWM) gating signals to switch the inverter. The comparator needs a sinusoidal modulating signal (Vm) and a triangular carrier signal (Vcr) to generate the IGBT gating signal (Vg) via bipolar switching. The comparator output is high (ON) when Vm is greater than Vcr and low otherwise. The waveform of the gating signal generation is shown in Fig. 3.

Hong Kong International Journal of Research Studies, ISSN: 3078-4018
Volume 3, Issue 2, July-December, 2025
Available online at:https://octopuspublication.com/index.php/hkijrs

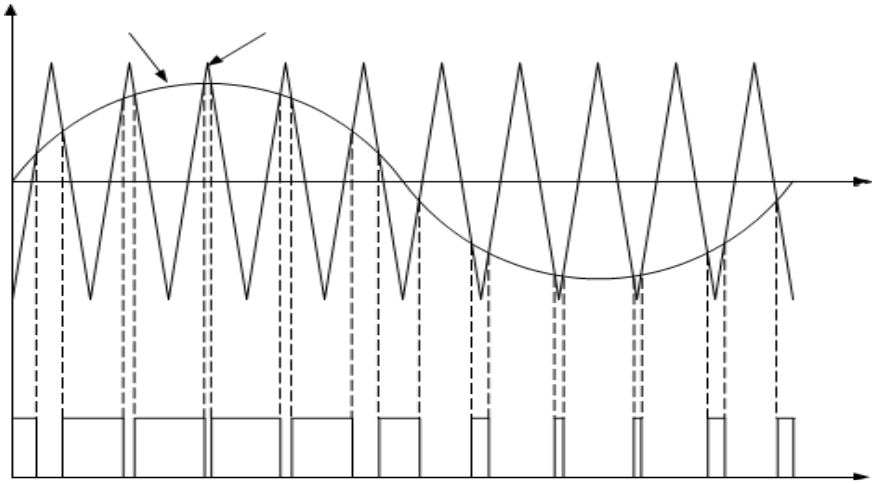

Figure 3: Vg generation

$M = \frac{A_m}{A_{cr}}$ ----------1

Where M = modulation index (decimal), A_m = amplitude of modulating signal (V) A_{cr} = amplitude of carrier signal (V)
The inverter output voltage phase depends on the Vm phase angle. Select the phase angle of Vm to match the grid current phase and achieve a unity power factor. The Vm frequency determines the inverter output voltage frequency. Inverter switching frequency (fs) depends on Vcr. In the created model, fm is set to 50 Hz to match the utility grid frequency, and fs is set to 10 kHz.

Operating outside the audible noise range usually requires switching frequencies of 20 kHz or more. As switching frequency increases, audible noise reduces [5]. Simulating high switching frequencies (20 kHz or more) requires a small simulation step size (µs or less) for accurate investigations, resulting in lengthy simulation times [6]. The simulation step size in this work is one µs.

Low-pass LC Filter Design
Inverter output voltage SPWM has harmonics. The maximum current output THD is 5%, per IEC 61727 (PV System, Characteristics of the Utility Interface). Thus, grid inverter design requires an LC filter. The LC filter must filter the switching frequency components of the inverter output current spectrum. The inverter circuit's output LC filter should create a sinusoidal output current with THD less than 5%.

Eq. (2) suggests that the low-pass LC filter's cut-off frequency, fc, should be higher than the grid frequency and lower than the inverter switching frequency. 1 kHz is the model's fc. We used 10 mH and 2.53 µF inductance and capacitance values for the LC filter.

$$f_c = \frac{1}{2\pi\sqrt{L_f C_f}} \quad \text{----------2}$$

Where,
fc = cut-off frequency (Hz) Lf = filter inductor (H), Cf = filter capacitor (F)

Grid Synchronization
The grid inverter needs a pure sinusoidal reference voltage to synchronize its sinusoidal output to the grid frequency. The inverter output voltage (Vinv) must surpass the grid voltage (Vgrid) to provide the grid with Iinv. See Fig. 4 for Vgrid, Vinv, Iinv, and voltage across the decoupling inductor (VXL) in the AC inverter equivalent circuit. The decoupling inductor, XL, controls power flow from the inverter to the grid.

Hong Kong International Journal of Research Studies, ISSN: 3078-4018
Volume 3, Issue 2, July-December, 2025
Available online at:https://octopuspublication.com/index.php/hkijrs

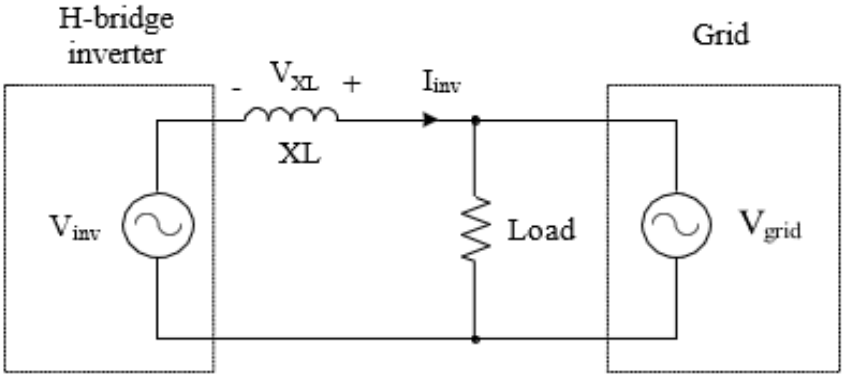

Figure 4: Equivalent circuit at the AC side of the inverter

In Fig. 5, the waveforms of Iinv and Vgrid must be in phase to achieve a unity power factor. In the phasor diagram, see Fig. 6. To align Iinv with Vgrid, Vinv must lead Vgrid with the angle (Fig. 6). Adjusting the modulating signal phase angle (Vm) does that.

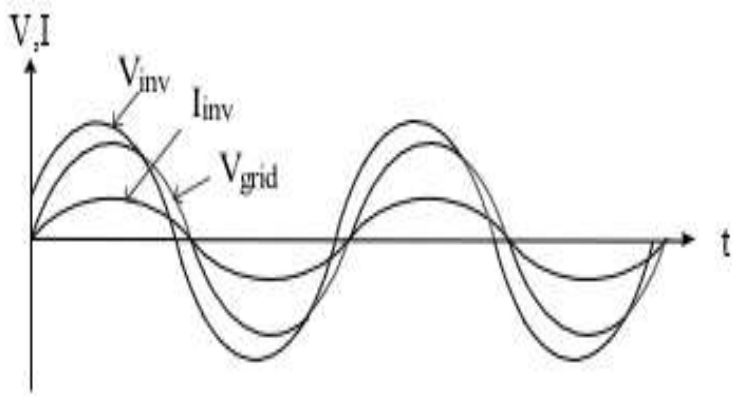

Figure 5: Waveforms of Vinv, Iinv, and Vgrid

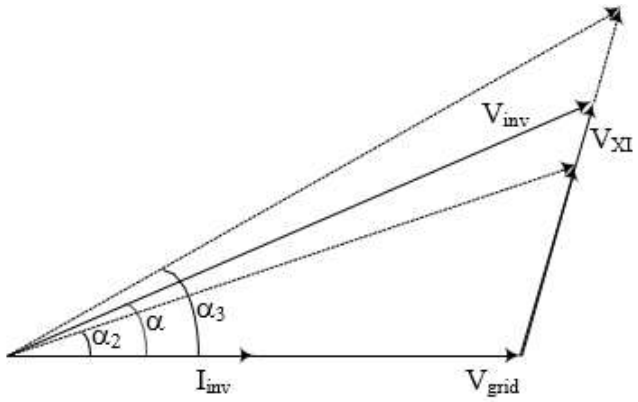

Figure 6: Vinv, Igrid, and Vgrid in phasor diagram

The phase angle of the modulating signal (Vm) is varied in response to solar irradiance and temperature levels to synchronize the Iinv with the Vgrid. The appropriate phase angle for a specific range of temperature and irradiance level must be set. In the developed model, the phase angle of Vm will automatically change to the appropriate value according to the range of cell temperature levels. For simplicity, since there is a quite linear relationship between solar irradiance and

cell temperature, the developed model will only detect the solar irradiance value for controlling the selection criteria of the phase angle value.

Simulation Work

Fig. 7 shows a circuit-based inverter model. IGBT switching signal generation is in the 'inverter switching' subsystem in Fig. 7 and the grid synchronization control subsystem in Fig. 8. The repeating sequence block generates a 10 kHz triangular carrier signal (Vcr). A 50-Hz sinusoidal AC voltage source block generates the sinusoidal modulating signal (Vm). Vg is produced by comparing Vcr and Vm with the relational operator. The 'NOT logical operator' block inverts Vg for inverter switching.

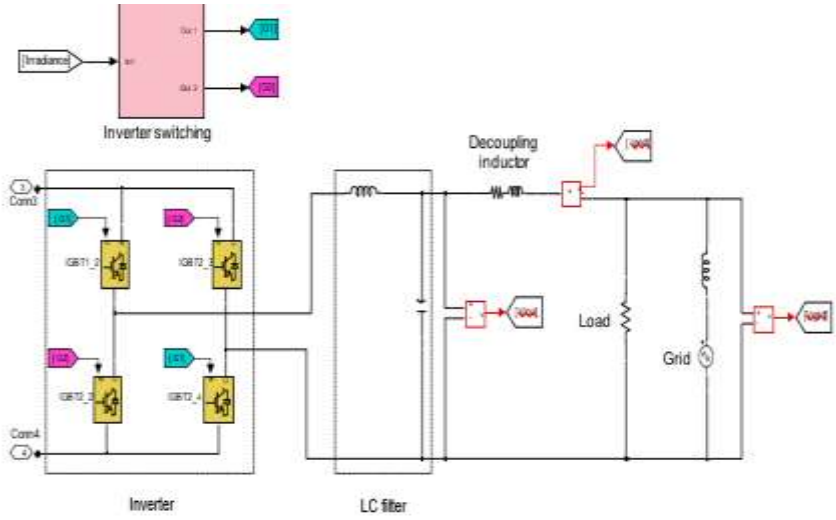

Figure 7: Inverter, LC filter, and utility grid circuit

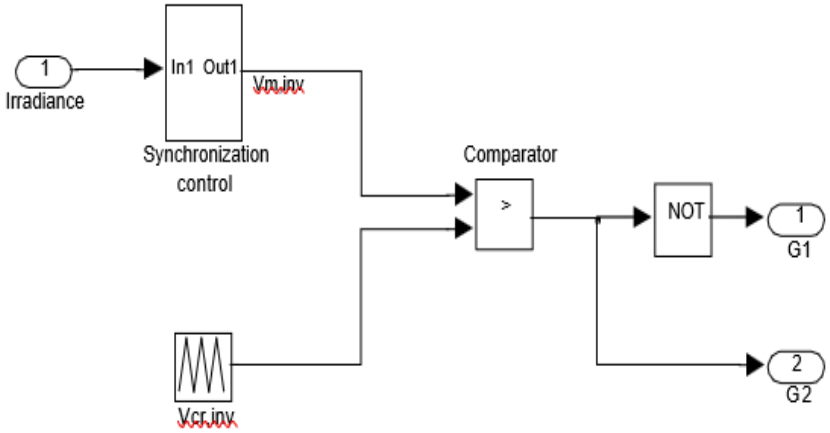

Figure 8: Inverter Switching Signal Generation

Fig. 8's synchronization control subsystem features many sinusoidal AC voltage source blocks with varying phases. A switch selects the AC voltage source block with the right phase value for grid synchronization. Using a lookup table, the source phase is chosen based on solar irradiation.

Low-pass LC filter on the inverter output. The two mH decoupling inductors are linked in series with the LC filter. In Fig. 7, a 5 Ω resistor acts as the load and is connected in parallel to the decoupling inductor. An AC voltage source block models the grid, while a one mH inductor in series with it works as a transmission line. Fig. 7's terminals 3 and 4 are the connections for the boost converter [4].

Hong Kong International Journal of Research Studies, ISSN: 3078-4018
Volume 3, Issue 2, July-December, 2025
Available online at:https://octopuspublication.com/index.php/hkijrs

RESULTS AND DISCUSSION

Without Consideration of De-rating Factors

First, examine the best case. Vinv, Vgrid, and Iinv measurement positions are shown in Fig. 9. Vinv is measured at the LC filter output. The transmission line, grid source, and decoupling inductor are used to measure the voltage (V) of the grid and the current (I) of the inverter (inv).

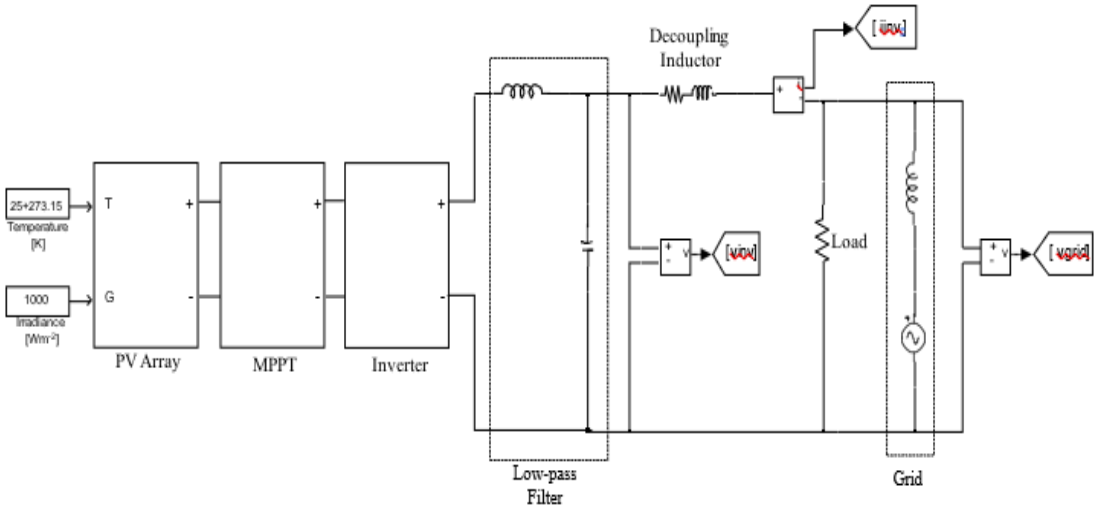

Figure 2:Measurement positions of Iinv, Vinv, and Vgrid

Fig. 10 displays the sinusoidal waveforms of the V grid and Iinv in the simulated model at a sun irradiation of 808 W/m² and a temperature of 69.51 °C. Inverter synchronization is indicated by the Iinv waveform being in phase with the V grid waveform. As shown in Fig. 11, the frequency spectrum of Iinv up to the 40th order of harmonics at G = 808 W/m² and T = 69.51°C was obtained using the Fast Fourier Transform Analysis tool in MATLAB Simulink software. The Iinv has a THD of 0.51% at T = 69.51°C and G = 808 W/m². Table 3 shows the Iinv THD for various sun irradiance inputs. The simulation shows that Iinv THD values for different solar irradiation levels are less than the IEC 61727 maximum of 5% [7].

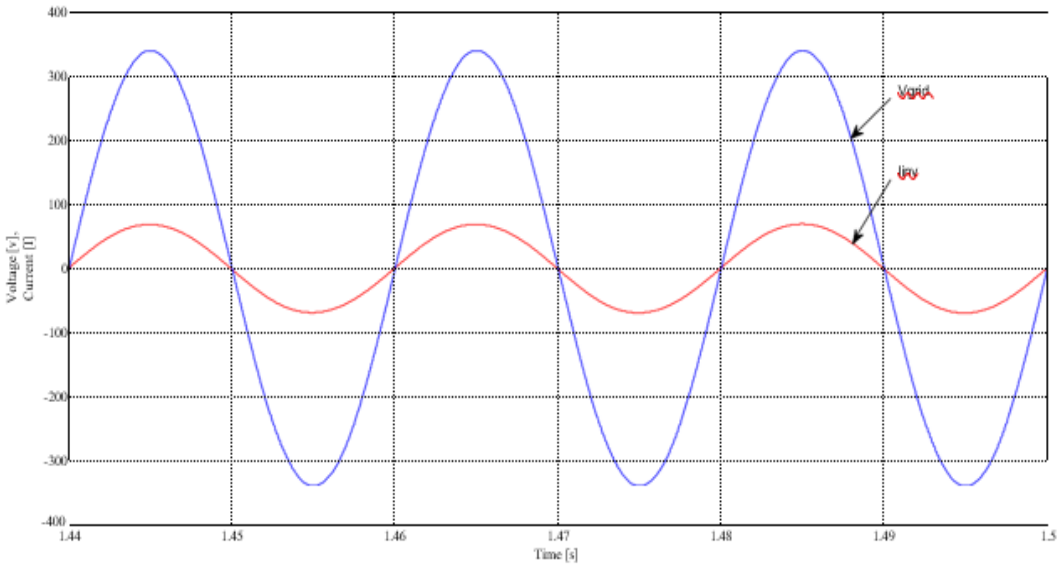

Figure 3: Waveforms of Iinv synchronized to Vgrid

Hong Kong International Journal of Research Studies, ISSN: 3078-4018
Volume 3, Issue 2, July-December, 2025
Available online at:https://octopuspublication.com/index.php/hkijrs

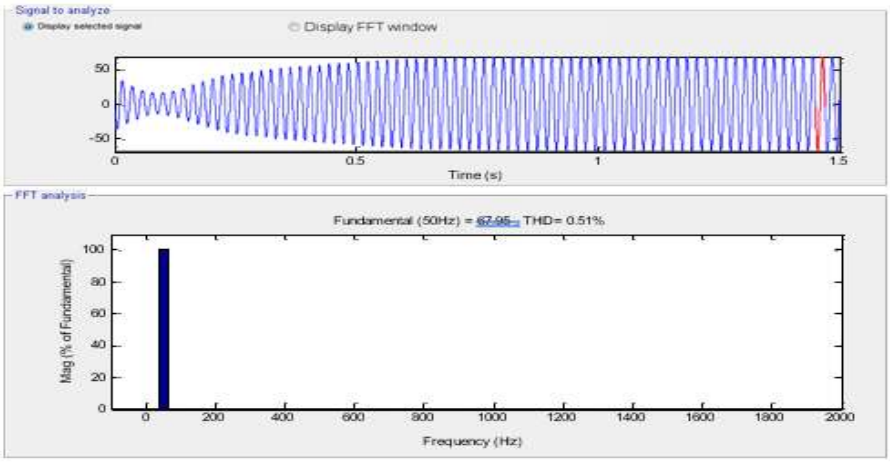

Figure 4: THD of Iinv at G=808 Wm² and T=69.61°C

Table 3: THD of Iinv for Varying Solar Irradiance Level

Irradiance (Wm²)	THD of Iinv
928	0.56
808	0.51
747	0.55
666	0.48
582	0.43

According to Eq. (3), AC power is the product of Iinv and Vgrid.
$Pac = Iinv \times Vgrid \times cos\emptyset$ ----------3
Where,

Pac = AC power (W), Iinv = inverter output current (A), Vgrid = grid voltage (V), and∅ = displacement angle (degrees).
Fig. 12 shows the simulation model's AC power and actual data for varied solar irradiance. Fig. 12 compares simulated and actual AC power. The simulation model's output AC power value has been multiplied by three to make it three-phase, permitting comparison with the data's three-phase power value. Fig. 12 shows that Pac_sim has more AC power than Pac_actual.

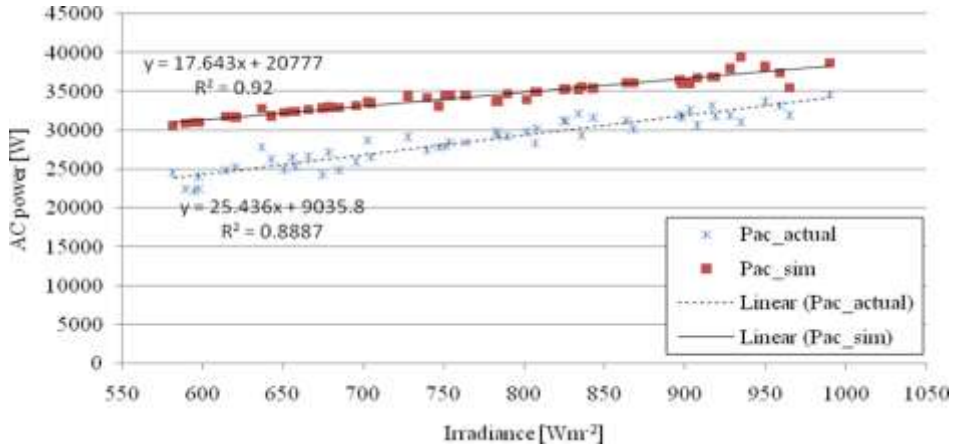

Figure 5: AC Output Power Against Solar Irradiance

Hong Kong International Journal of Research Studies, ISSN: 3078-4018
Volume 3, Issue 2, July-December, 2025
Available online at:https://octopuspublication.com/index.php/hkijrs

RMSE and MAPE are used to compare simulated and actual output. As described in Eq. (4), the RMSE is often used to compare model simulations to absolute system values. The computed RMSE is in watts (W). MAPE, presented as a percentage, measures the accuracy of fitted time series values. As stated in Eq. (5), MAPE averages the absolute values of all percentage errors. MAPE is beneficial for reporting since it uses generic percentage terms that most consumers can understand. Pac_sim before Pac_actual has 5,920.646 W RMSE and 20.744% MAPE.

$$RMSE = \sqrt{\frac{\sum_{i=1}^{n} (P_{actual\_i} - P_{sim\_i})^2}{n}}$$

----------4

Where,Pactual_i = actual power, Psim_i = simulated power, n = number of samples

Consider De-Rating Factors

In practice, a grid-connected PV system cannot transfer the full electricity from the PV array into the grid. Due to manufacturing tolerances, module mismatch losses (MML), cable losses (CL), PV module dirt (DPM), and inverter efficiency, PV systems experience losses of electricity. Table IV displays the values of □ inv, fmm, fdirt, and fcable utilized in the model simulation. For fmm and □ inv values, consult the PV module and inverter datasheets. Multiple studies have assumed fdirt and fcable values depending on Malaysia's climate and rainfall frequency [8].

Table 4:De-Rating Factors

De-rating factors	Values
$\eta_{inv,}$	0.943
f_{dirt}	0.970
f_{cable}	0.980
f_{mm}	0.950

The simulated output power must be multiplied by fmm, fdirt, fcable, and ηinv, as indicated in Table 4. In actuality, specific characteristics are challenging to estimate precisely, including the dirt factor, module mismatch, and cable loss.

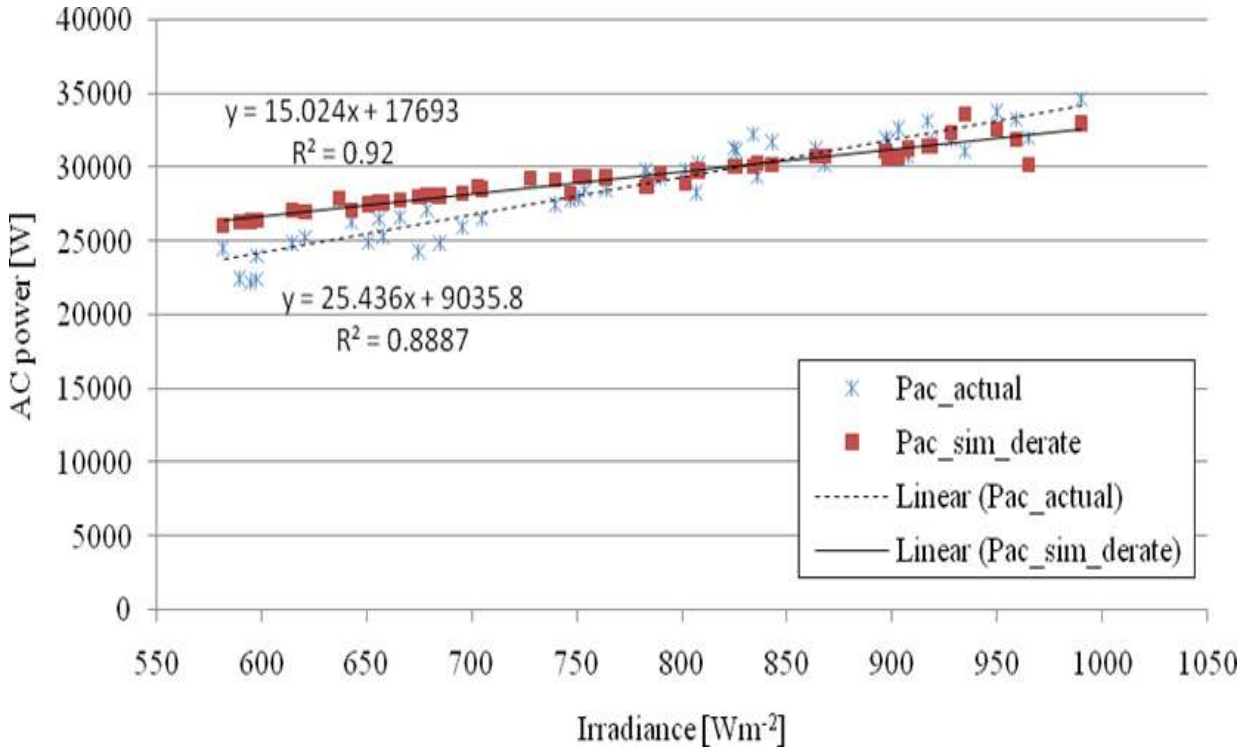

Figure 13: AC output power with consideration of de-rating factors against solar irradiance

CONCLUSION

We developed and demonstrated a single-phase full-bridge inverter for grid-connected PV power systems. The inverter output current THD is below the maximum for variable solar irradiation input. Single-phase full-bridge inverters for grid THD are allowed at 5% under the IEC 61727 standard. We compare the inverter output power to the actual AC power using RMSE and MAPE. The grid voltage and inverter output current are synchronized. Take into account fmm, fdirt, fcable, and inv at the simulation output for more precise results. These de-rating variables reduce DC and AC RMSE and MAPE.

The circuit-based model helps explain the electrical behavior of grid-connected PV system devices within the circuit. It is used in power electronics simulations. Improved synchronization control could enhance the model. Solar irradiation and temperature must be considered when selecting Vm phase angles to obtain a proper output power value.

REFERENCES

[1] S. Shaari, A. M. Omar, A. H. Haris, and S. I. Sulaiman, Solar Photovoltaic Power: Fundamentals: Ministry of Energy, Green Technology and Water, Malaysia/Malaysia Building Integrated Photovoltaic Project, 2010.
[2] S. B. Kjaer, J. K. Pedersen, and F. Blaabjerg, "A review of single-phase grid-connected inverters for photovoltaic modules," Industry Applications, IEEE Transactions on, vol. 41, pp. 1292-1306, 2005.
[3] M. Calais, J. Myrzik, T. Spooner, and V. G. Agelidis, "Inverters for single-phase grid-connected photovoltaic systems—an overview," in Power Electronics Specialists Conference, 2002. pesc 02. 2002 IEEE 33rd Annual, 2002, pp. 1995-2000.
[4] H. M. Nordin and A. M. Omar, "Modeling and simulation of photovoltaic (PV) array and maximum power point tracker (MPPT) for grid-connected PV system," in Sustainable Energy & Environment (ISESEE), 2011 3rd International Symposium & Exhibition, pp. 114-119.
[5] Malfait, R. Reekmans, and R. Belmans, "Audible noise and losses in variable speed induction motor drives with IGBT inverters—influence of the squirrel cage design and the switching frequency," in Industry Applications Society Annual Meeting, 1994, Conference Record of the 1994 IEEE, 1994, pp. 693-700vol. 1.
[6] M. H. Nehrir and C. Wang, Modeling and Control of Fuel Cells: Distributed Generation Applications, John Wiley & Sons, 2009.

[7] "Photovoltaic (PV) systems—Characteristics of the utility interface," in IEC 61727, 2004.
[8] S. Shaari, A. M. Omar, A. H. Haris, and S. I. Sulaiman, Solar photovoltaic power: testing, commissioning, and acceptance test of grid-connected systems: Ministry of Energy, Green Technology, and Water Malaysia/MBIPV Project, 2010.